Nuclear Physics A567 (1994) 553–575
North-Holland

NUCLEAR
PHYSICS A

Spontaneous symmetry breaking in a solvable nuclear model

D.B. Stout

Divison de Physique Théorique, I.P.N. 91406 Orsay Cedex, France

Received 18 February 1993
(Revised 10 May 1993)

Abstract

We show that non-perturbative effective interaction techniques can be applied to the $1/N \to 0$ limit of the pairing Lipkin model to yield an apparently exact solution. Results at finite N allow us to study the reliability of the random phase and related approximations. This model which is very similar in behavior to the Gross–Neveu model allows us to make interesting observations about the effect of tunneling on discrete symmetry "Goldstone" degeneracies. This analysis is also interesting from the many-body point of view as our method avoids the occurrence of RPA instability at large values of the coupling constant and at least in the present model we see that such an "instability" indicates a $N \to \infty$ limit phase transition.

1. Introduction

In this work we solve the $1/N \to 0$ limit of the pairing Lipkin model [1] using a combination of effective potential and RPA techniques. This model contains a discrete symmetry between particle and hole states. Hartree–Fock analysis predicts that this symmetry is spontaneously broken for sufficiently large coupling, the well-known deformed Hartree–Fock potential [2]. In the present work we show that the spontaneous symmetry breaking can be conveniently treated by effective interaction techniques which when combined with RPA apparently achieve an exact solution to the problem including a phase transition in the $N \to \infty$ limit.

In addition, finite-N results provide interesting observations about the effect of tunneling on the degeneracies induced by the spontaneous breaking of the discrete symmetry. The principle difference being that in the $N \to \infty$ limit, a shifted single-particle spectrum (the non-relativistic analogue of a mass shift) occurs only when the interaction coupling is sufficiently large to produce SSB (spontaneous symmetry breaking). At finite N however, the single-particle spectrum is shifted for all values of the coupling. Witten found evidence of a related phenomenon for a continuous symmetry in the SU(N) Thirring model [3]. Thus the finite-N

SSDI 0375-9474(93)E0412-2

Thirring model has fermion mass generation even when the symmetry is not spontaneously broken.

Subsequent publications will concern treatments of the fluctuations (i.e. correlation energy at finite-N and other $1/N$ corrections). The motivation for using the Lipkin model in the present work was to find a system where the $1/N$ expansion could be studied in comparison with exact results. We stress that the techniques developed here can be generalized to more complicated systems, but for the sake of clarity in the discussion of spontaneous symmetry breakdown, we largely limit the discussion to the Lipkin model example.

Also, we wish to emphasize that we did not simply make a boson approximation in the current work. That is we took care to insure that our formulae contain exchange terms. Although such considerations are irrelevant in the $N \to \infty$ limit, they should be included if we are to make serious attempts at calculating $1/N$ corrections.

In the next section we derive RPA in a Feynman diagram context and discuss several important RPA features such as its role in $1/N$ expansions, RPA "breakdown", and RPA normalization. The reader familiar with RPA lore may in principle skip this section although the somewhat "novel" derivation of RPA normalization may prove of interest. In sect. 3 we calculate the effective potential in the pairing Lipkin model using recently derived summation techniques. In sect. 4 we compare the combined RPA – effective potential analysis to exact results. Finally in sect. 5 we address other physical quantities such as binding energy and the single-particle spectrum.

2. A derivation of RPA via Feynman diagrams

There exists a variety of RPA derivations throughout the literature. In nuclear physics the most common arises from the linearization of the equations of motion. In this section we derive the RPA for discrete systems in a Green function context using the alternative language of Feynman diagrams. The advantage of this method is that it employs standard field theory techniques such as Feynman diagrams and Dyson equations. It even yields the sometimes obscure RPA normalization in a fashion analogous to wave-function normalization *.

As usual in many-body physics, we assume our hamiltonian has the form $H = H_0' + V$, where H_0' is a one-body hamiltonian and V is a two-body interaction i.e.

$$H = H_0' + V = \sum_{\alpha} \varepsilon_{\alpha} a_{\alpha}^{\dagger} a_{\alpha} + \tfrac{1}{4} \sum_{\alpha,\beta,\gamma,\delta} \bar{V}_{\alpha\beta,\gamma\delta} a_{\alpha}^{\dagger} a_{\beta}^{\dagger} a_{\delta} a_{\gamma}. \tag{1}$$

* To be precise, RPA normalization appears as particle–hole wave-function normalization.

We follow the convention that V is an operator while $\bar{V}_{\alpha\beta,\gamma\delta}$ is an antisymmetrized matrix element of V i.e.

$$\bar{V}_{\alpha\beta,\gamma\delta} = V_{\alpha\beta,\gamma\delta} - V_{\alpha\beta,\delta\gamma}, \tag{2}$$

where

$$V_{\alpha\beta,\gamma\delta} = (\alpha\beta|V|\gamma\delta), \tag{3}$$

$|\alpha\beta)$ representing a fermionic product state occupying single-particle states α and β. As usual, H_0', is viewed as the "unperturbed" interaction. We thus build our perturbation theory around an N-particle closed-core ground state $|c_N\rangle$, which is the lowest-energy Slater-determinant ground state of the unperturbed hamiltonian, H_0'.

For sake of notational convenience we define a shifted one-body hamiltonian, H_0, such that

$$H_0 \overset{\text{def}}{=} H_0' - \langle c|H_0'|c\rangle = H_0' - \epsilon_0^N, \tag{4}$$

where ϵ_N^0 is the unperturbed ground-state energy. With this definition, the single-particle single-hole energies of H_0 have the Landau–Migdal definition of quasi-particle energy for an N-particle system. That is to say, we can write the one-body hamiltonian as $H_0 = H_0^{\mathrm{p}} - H_0^{\mathrm{h}}$, H_0^{p} having the property that

$$H_0^{\mathrm{p}} a_m^\dagger |c\rangle = \varepsilon_m a_m^\dagger |c\rangle = \left(\epsilon_m^{N+1} - \epsilon_0^N\right) a_m^\dagger |c\rangle, \tag{5}$$

where ϵ_m^N denotes the energy (using hamiltonian H_0) of the mth state of the $N+1$-body system. The hole hamiltonian has analogous properties

$$H_0^{\mathrm{h}} a_i |c\rangle = \varepsilon_i a_i |c\rangle = \left(\epsilon_0^N - \epsilon_i^{N-1}\right) a_i |c\rangle. \tag{6}$$

Thus the ith single-hole energy is the energy of the N-particle ground state minus the energy of the ith $N-1$ particle state.

We now define the bare (i.e. unperturbed) single-particle Green function as

$$f_{\alpha\beta}(t) \overset{\text{def}}{=} \theta(t)\langle c|a_\alpha(t)a_\beta^\dagger(0)|c\rangle - \theta(-t)\langle c|a_\beta^\dagger(0)a_\alpha(t)|c\rangle, \tag{7}$$

using interaction-picture creation and destruction operators.

The unperturbed particle–hole Green function is likewise defined

$$\begin{aligned}\left[F_{\mathrm{b}}(t)\right]_{mi,nj} &\overset{\text{def}}{=} \theta(t)\langle c|a_i^\dagger(t)a_m(t)a_n^\dagger(0)a_j(0)|c\rangle \\ &\quad + \theta(-t)\langle c|a_j^\dagger(0)a_n(0)a_m^\dagger(t)a_i(t)|c\rangle \\ &\overset{\text{def}}{=} \left[F_{\mathrm{b}}^-(t)\right]_{mi,nj} + \left[F_{\mathrm{b}}^+(t)\right]_{mi,nj},\end{aligned} \tag{8}$$

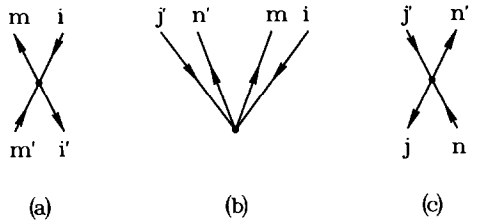

Fig. 1. Diagrams taking part in the RPA: (a) particle–hole interaction proceeding forward in time, (b) backward-time particle–hole state undergoing interaction to begin propagating forward in time, (c) particle–hole interaction proceeding backward in time.

where m, n are used here and throughout to denote particle states while i, j are used to denote hole states. $F_b^+(t)$ and $F_b^-(t)$ are known respectively as the advanced and retarded particle–hole Green functions. An equivalent definition of F_b is

$$F_b(t) = -f(t)f(-t). \tag{9}$$

Now we switch on the two-particle interaction operator V. We define particle–hole matrix elements (shown diagrammatically in Fig. 1a) as

$$A_{m,i;m',i'} \overset{\text{def}}{=} \langle mi \,|\, V \,|\, m'i' \rangle = \langle c \,|\, a_i^\dagger a_m V a_{m'}^\dagger a_{i'} \,|\, c \rangle = -V_{mi',m'i}. \tag{10}$$

In order to include ground-state correlations, we will include another class of interactions

$$B_{m,i;n',j'} \overset{\text{def}}{=} \langle mi;\ nj \,|\, V \,|\, c \rangle = \langle c \,|\, a_i^\dagger a_m a_{j'}^\dagger a_{n'} V \,|\, c \rangle = V_{mn,ij} \tag{11}$$

(shown in Fig. 1b), and its complex conjugate $B^\dagger$. We see that the B interaction may be viewed as that between a particle–hole state propagating forward in time and one propagating backward in time. The particle–hole states propagating backward in time may also undergo interactions *, so we also introduce the matrix operator

$$A^*_{n',j';n,j} \overset{\text{def}}{=} \langle n'j' \,|\, V \,|\, nj \rangle = \langle c \,|\, a_{j'}^\dagger a_{n'} V a_n^\dagger a_j \,|\, c \rangle = -V_{n'j,j'n} \tag{12}$$

(shown in Fig. 1c).

* Depending on the physical problem considered, the space spanned by n, j may or may not be the same as that spanned by m, i.

With these definitions, we are now ready to derive the RPA equation. We begin by considering a retarded bare particle–hole propagator

$$[F_b^-(\omega)]_{mi,nj} = \delta_{m,n}\delta_{i,j}\frac{1}{\omega - \varepsilon_m + \varepsilon_i + i0^+}, \tag{13}$$

where as always in this work, the 0^+ implies an arbitrarily small positive real number. In the following discussion we will find it convenient to write this in a matrix form with particle–hole indices suppressed i.e.

$$F_b^-(\omega) = \frac{1}{\omega - H_0 + i0^+}. \tag{14}$$

We now begin to construct an approximation to the full particle–hole Green function. It is clear that we should include interactions between the forward-going particle–hole pairs. Summing these (ladder diagrams) to all orders yields

$$F^-(\omega) \overset{\text{def}}{=} F_b^-(\omega) + F_b^-(\omega)AF_b^-(\omega) + \ldots = \frac{1}{\omega - H_0 - A + i0^+}, \tag{15}$$

where the matrix elements of A are given by (10). The same thing could be done for the advanced propagator to yield

$$F^+(\omega) = -\frac{1}{\omega + H_0 + A^* - i0^+}. \tag{16}$$

Rather than stop here, we note another type of diagram which should be included. Consider a forward propagating particle–hole state which interacts through $B^\dagger$, propagates backwards in time, then interacts through B to propagate forward in time again. The backward-going particle–hole lines may interact through A^* so we use the advanced propagator in (16) for these lines. We will call this interaction the RPA interaction defined

$$V_{\text{RPA}}(\omega) \overset{\text{def}}{=} -B\frac{1}{\omega + H_0 + A^* - i0^+}B^\dagger. \tag{17}$$

We may sum interactions of this type to all orders using a Dyson equation where our approximation to the true Green function is defined

$$G(\omega) = F^-(\omega) + F^-(\omega)V_{\text{RPA}}(\omega)G(\omega). \tag{18}$$

The reader should note that this Green function is defined on the m, i states (i.e. forward-going) particle–hole space.

Using (15), (17), and (18) we find

$$\{G(\omega)\}^{-1} = \omega - H_0 - A + B\frac{1}{\omega + H_0 + A^* - i0^+}B^\dagger$$

$$\stackrel{\text{def}}{=} \omega - \mathscr{H}_{\text{ph}}(\omega), \tag{19}$$

where $\mathscr{H}_{\text{ph}}(\omega)$ for reasons which will become clear below is referred to as the particle–hole (energy dependent) "effective" hamiltonian.

In principle if A, A^*, and B contained all possible diagrams without overcounting then (19) would be an exact result. The random-phase "approximation" then is just to consider the contributions to A, A^*, and B given by (10)–(12).

When we extract physical results, we recall that we are trying to approximate the exact Green function. The exact Green function has a Fourier transform

$$G^{\text{exact}}_{\alpha'\beta',\alpha\beta}(\omega) = \sum_m \frac{\langle\Psi_0|a^\dagger_{\beta'}a_{\alpha'}|\Psi_m\rangle\langle\Psi_m|a^\dagger_\alpha a_\beta|\Psi_0\rangle}{\omega - (E_m - E_0) + i0^+}$$

$$- \frac{\langle\Psi_0|a^\dagger_\alpha a_\beta|\Psi_m\rangle\langle\Psi_m|a^\dagger_{\beta'}a_{\alpha'}|\Psi_0\rangle}{\omega + (E_m - E_0) - i0^+}, \tag{20}$$

where E_α represents an eigenstate of the full hamiltonian for the N-particle system. Thus we see that since (19) is an approximation to the exact Green function, the poles of $G(\omega)$ should be identified as the physical spectrum found in the denominator of (20). Using (19) we see that the poles of $G(\omega)$ are given by the self-consistent eigenvalues of the effective hamiltonian i.e.

$$\mathscr{H}_{\text{ph}}(E^\alpha_{\text{ph}})x^\alpha \equiv H_0 x^\alpha + Ax^\alpha - B\frac{1}{E^\alpha_{\text{ph}} + H_0 + A^* - i0^+}B^\dagger x^\alpha$$

$$= E^\alpha_{\text{ph}} x^\alpha, \tag{21}$$

where x^α is a vector in the particle–hole space. From the remarks made above we have

$$E^\alpha_{\text{ph}} \approx E_\alpha - E_0. \tag{22}$$

Thus we see that the self-consistent solutions to our "effective" hamiltonian acting within the particle–hole space give the excitation spectrum of the full hamiltonian.

Eq. (21) may be easily solved by use of a simple trick, i.e. we define a vector y^α in the backward-going space (n, j),

$$y^\alpha \stackrel{\text{def}}{=} -\frac{1}{E^\alpha_{\text{ph}} + H_0 + A^* - i0^+}B^\dagger x^\alpha. \tag{23}$$

With this definition (21) is written

$$H_0 x^\alpha + A x^\alpha + B y^\alpha = E^\alpha_{\rm ph} x^\alpha, \tag{24}$$

while the definition in (23) may be expressed

$$-H_0 y^\alpha - A^* y^\alpha - B^\dagger x^\alpha = E^\alpha_{\rm ph} y^\alpha. \tag{25}$$

Putting these together, we have an eigenvalue equation

$$\begin{pmatrix} H_0 + A & B \\ -B^\dagger & -H_0 - A^* \end{pmatrix} \begin{bmatrix} x^\alpha \\ y^\alpha \end{bmatrix} = E^\alpha_{\rm ph} \begin{bmatrix} x^\alpha \\ y^\alpha \end{bmatrix}. \tag{26}$$

Thus our solution for the physical spectrum is the eigenvalue spectrum of this matrix, usually called the RPA matrix. Frequently in physical problems, the particle–hole space for backward-going lines is identical to that of the forward-going lines; in this case the RPA matrix can take the symmetric form

$$\begin{pmatrix} H_0 + A & B \\ -B & -H_0 - A \end{pmatrix} \begin{bmatrix} x^\alpha \\ y^\alpha \end{bmatrix} = E^\alpha_{\rm ph} \begin{bmatrix} x^\alpha \\ y^\alpha \end{bmatrix}, \tag{27}$$

where A and B can be taken as real symmetric matrices. We note that as expected from the true Green function, the symmetric form has the property that if $E^\alpha_{\rm ph}$ is a solution, then $-E^\alpha_{\rm ph}$ is also a solution.

Upon inspection, we note that our RPA matrices (26) and (27) do not tell us the proper normalization of the RPA eigenvector. A properly normalized eigenvector however contains important physical information. Looking at the residues of the exact Green function, (20), we realize that

$$\begin{aligned} \langle \Psi_\alpha | a^\dagger_m a_i | \Psi_0 \rangle &\overset{\rm def}{=} X^\alpha_{mi} \propto x^\alpha_{mi}, \\ \langle \Psi_\alpha | a^\dagger_i a_m | \Psi_0 \rangle &\overset{\rm def}{=} Y^\alpha_{mi} \propto y^\alpha_{mi}. \end{aligned} \tag{28}$$

As we do not yet know the value of the physical eigenvector, X^α, let us choose for convenience $|x^\alpha| \overset{\rm def}{=} \sum_{mi} |x^\alpha_{mi}|^2 = 1$, and calculate the renormalization constant relating the two. With our chosen x^α normalization, and (19), we find the residue at the pole of the retarded Green function is

$$Z^\alpha_{\rm ph} = \frac{1}{\langle x_\alpha | 1 - (\mathrm{d}/\mathrm{d}\omega) \mathscr{K}_{\rm ph}(\omega) |_{\omega = E^\alpha_{\rm ph}(\omega)} | x_\alpha \rangle}, \tag{29}$$

which is essentially that of Hengeveld et al. [4]. Under the assumption that H_0, A, and B are energy independent and using the definitions in (19) and (23), we see that this can be rewritten as

$$Z^{\alpha}_{\mathrm{ph}} = \frac{1}{1-|y^{\alpha}|^2}. \tag{30}$$

The properly normalized transition vector is thus

$$X^{\alpha} = \left(Z^{\alpha}_{\mathrm{ph}}\right)^{1/2} x^{\alpha}. \tag{31}$$

As y^{α} is linearly dependent upon x^{α}, it should be similarly rescaled such that

$$Y^{\alpha} = \left(Z^{\alpha}_{\mathrm{ph}}\right)^{1/2} y^{\alpha}. \tag{32}$$

Using the relation in (30) and $|x^{\alpha}| = 1$, it is clear that the properly renormalized physical amplitudes X^{α} and Y^{α} satisfy

$$|X^{\alpha}|^2 - |Y^{\alpha}|^2 = 1, \tag{33}$$

yielding the familiar RPA normalization condition.

We should note however that in nuclear physics the "hard core" of the nuclear potential necessitates that short-range correlations be taken into account by replacing the bare interaction with a Brueckner G-matrix. Contrary to the assumption made in deriving (30), the G-matrix is in principle energy dependent. More importantly, Allart and coworkers [4,5] have shown that one obtains improved description of nuclear properties by simultaneously including self-energy contributions to the single-particle hamiltonian H_0 and additional core polarization diagrams in the particle–hole interactions of the A and B matrices (ex. including couplings to 2p2h states). Corrections to the B matrix can be rendered energy dependent while corrections to A and self-energy terms are energy dependent. Thus in general, the excitation spectrum derived from (21) are the self-consistent solutions, $\omega = E^{\alpha}_{\mathrm{ph}}(\omega)$, of the energy-dependent RPA matrix

$$\begin{pmatrix} H_0 + A(\omega) & B \\ -B & -H_0 - A(-\omega) \end{pmatrix} \begin{bmatrix} x^{\alpha} \\ y^{\alpha} \end{bmatrix} = E^{\alpha}_{\mathrm{ph}}(\omega) \begin{bmatrix} x^{\alpha} \\ y^{\alpha} \end{bmatrix}, \tag{34}$$

where for notational convenience we take H_0 to be an energy-independent mean field and associate the energy-dependent self-energy corrections with the A matrix corrections. Carrying through the same analysis as above for the energy-dependent

RPA matrix, (34), we find that the RPA normalization for the properly normalized vectors now denoted $\mathscr{X}$ and $\mathscr{Y}$ is

$$|\mathscr{X}^{\alpha}|^2 - |\mathscr{Y}^{\alpha}|^2 = \frac{1}{1 - (\mathrm{d}/\mathrm{d}\omega)E^{\alpha}_{\mathrm{ph}}(\omega)\big|_{\omega = E^{\alpha}_{\mathrm{ph}}(\omega)}}, \tag{35}$$

as recently derived by Yang and Kuo [6]. In the current work, we only consider calculations of lowest order in the $1/N$ expansion, and we will see that ordinary RPA with normalization (33) will precisely yield this term. Inclusion of diagrams of higher orders in the $1/N$ expansion would however create energy dependencies and thus necessitate the use of the corrected normalization of (35).

We are now in a position to see some of the possible pitfalls of RPA. The poles of the exact Green function occur at real ω. The RPA matrix equation which purports to calculate these poles, (27) or (34), is non-hermitian and thus given appropriate values of the matrix elements can generate complex eigenvalues. When such conditions occur in the course of calculations it is often said that the RPA solution is "unstable" or has "broken down".

Another problem has recently been discussed at length by Kuo and collaborators. That is, given the general structure of the RPA equation, it can be shown [7] that the normalizations of the physical amplitudes (see Eqs. (28) and (33)) diverge at the point of onset of complex eigenvalues. In view of (28), a divergent RPA normalization is clearly pathological for a *finite* system.

To understand the "breakdown" of RPA we must ask ourselves why RPA should be a good approximation in the first place. Although it does sum a class of Feynman diagrams to all orders, there is a large number of diagrams to each order that are ignored by the RPA. The reasoning becomes clear when we regard the diagrammatic structure. RPA sums up all diagrams of the form shown in Fig. 2, where each dot represents an interaction integrated over all possible time orderings. The dots for a particular graph thus may represent A, A^*, B or $B^{\dagger}$ depending on the time ordering of a particular graph while summing over all possible time orderings.

We now note that in each loop of Fig. 2, we must sum over all possible particle–hole states. Upon inspection, we readily see that RPA sums in each order of perturbation theory those particle–hole diagrams containing the largest number

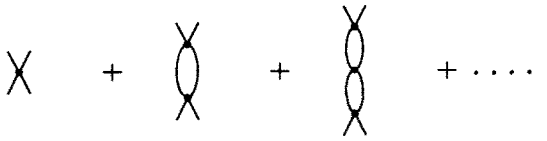

Fig. 2. Feynman diagrams contributing to the RPA approximation of the true Green function. The interaction is denoted by a dot. All possible time orderings are summed.

of loops. Thus we expect RPA to be a good approximation if there is a large number of degenerate or nearly degenerate intermediate particle–hole states, thus making the maximum loop diagrams much larger order by order than the diagrams containing fewer loops. For example, in the N-particle Lipkin model introduced in the next section, each loop in the RPA expansion is weighted by a factor $(N-1)$. Thus as we will see in sect. 4, RPA is equivalent in the Lipkin model to the lowest order in the $1/N$ expansion of the particle–hole propagator.

We now see that our worries stated above concerning the divergence of RPA eigenvector normalization no longer holds as the number of particle–hole states $\to \infty$. If the number of particle–hole states $\to \infty$ then the normalization of the RPA eigenvector, $|X^{\alpha}|$, may indeed $\to \infty$ while individual matrix elements, (28), remain finite. This argument may relieve our worries about RPA normalization, but does not appear to help us understand the appearance of complex RPA eigenvalues. As will be demonstrated in the following sections for the Lipkin model however, the stability of RPA will depend on the proper choice of unperturbed ground state.

From here on we will leave the general case and limit our discussion to the Lipkin model. Essentially all of the formulae which follow can be generalized to more complex systems, but the derivations and symmetry-breaking analysis will be more transparent if not buried beneath formalism.

3. An effective potential for the Lipkin model

In this section we show how auxiliary fields similar to those employed in relativistic field theory treatments of four-point interactions may be introduced to the Lipkin many-body hamiltonian. As in the Gross–Neveu model, the Lipkin model contains a discrete symmetry, and the vacuum expectation value of an auxiliary field (defined below) will serve as an order parameter for the spontaneous breaking of this symmetry. As is common in such theories an effective potential based on the auxiliary field will be used to probe for instabilities in the perturbative (i.e. symmetric) ground state.

The pairing Lipkin model has the following simple form. We take one shell of energy $\frac{1}{2}\varepsilon$ lying above the Fermi surface with spin j and another shell of energy $-\frac{1}{2}\varepsilon$ and spin j lying below. We address the case of $N = 2j+1$ particles. The unperturbed ground state thus has all particles lying in the lower shell. The unperturbed hamiltonian is written

$$\hat{H}_0 = \tfrac{1}{2}\varepsilon \sum_m \left(a^{\dagger}_{+,m} a_{+,m} - a^{\dagger}_{-,m} a_{-,m}\right), \tag{36}$$

while the two-body interaction has the form

$$\hat{V} = -\tfrac{1}{2}\lambda\left[\sum_m a^\dagger_{+,m}a_{-,m}\right]\left[\sum_{m'} a^\dagger_{+,m'}a_{-,m'}\right] + \text{h.c.} \tag{37}$$

$$= -\tfrac{1}{2}N\lambda\left[\sum_m C^{j,j,0}_{m,-m,0}(-)^{j-m}a^\dagger_{+,m}a_{-,m}\right]\left[\sum_{m'} C^{j,j,0}_{m',-m',0}(-)^{j-m'}a^\dagger_{+,m'}a_{-,m'}\right]$$

$$+ \text{h.c.}, \tag{38}$$

where λ is a positive real number (We lose no generality in this choice since the eigenspectrum for this model depends only on $\lambda^*\lambda$.) The interaction in (38) is written in angular-momentum coupled form to stress that the interaction is amongst particle–hole pairs coupled to zero angular momentum.

We now note that the hamiltonian transforms $H \to -H$ under the discrete symmetry transformation

$$a_{\pm,m} \to a_{\mp,m}, \qquad a^\dagger_{\pm,m} \to a^\dagger_{\mp,m} \tag{39}$$

(we have made use of the fact that the sign λ is arbitrary). It is this symmetry which we expect to be susceptible to spontaneously breaking.

In this model there is no direct interactions of the form (10) or (12), but we do have a turn-around interaction (and its complex conjugate) of the form found in (11):

$$B_{+-,+-} = -(N-1)\lambda \overset{\text{def}}{=} -v. \tag{40}$$

We note that had we just included the direct terms we would have had $B_{+-,+-} = -N\lambda$, and that the additional λ comes from including the exchange interaction which here corrects for the presence of Pauli violating terms in $\hat{V}$ of the form $a^\dagger_{+,m}a_{-,m}a^\dagger_{+,m}a_{-,m}$.

We take the field theory example and rewrite the hamiltonian in an equivalent form (i.e. having the same equations of motion). That is, we introduce $2N(N-1)$ auxiliary fields to the hamiltonian

$$H \to H + \sum_{m,m'}{}' \left(\frac{\sigma_{m,m'}\sqrt{2}}{\sqrt{\lambda}} - \frac{\sqrt{\lambda}}{2\sqrt{2}}\left[a^\dagger_{+,m}a_{-,m} + a^\dagger_{+,m'}a_{-,m'}\right]\right)^2$$

$$+ \sum_{m,m'}{}' \left(\frac{\sigma^*_{m,m'}\sqrt{2}}{(\sqrt{\lambda})} - \frac{\sqrt{\lambda}}{2\sqrt{2}}\left[a^\dagger_{-,m}a_{+,m} + a^\dagger_{-,m'}a_{+,m'}\right]\right)^2, \tag{41}$$

where the prime on the summation tells us that terms $m = m'$ are not included in the sum. As in field theory the auxiliary fields do not have true equations of

motion but instead obey constraint equations which result in the expectation-value relations

$$\langle \sigma_{m,m'} \rangle = \tfrac{1}{4}\lambda \langle [a^{\dagger}_{+,m} a_{-,m} + a^{\dagger}_{+,m'} a_{-,m'}] \rangle$$
$$\langle \sigma^{*}_{m,m'} \rangle = \tfrac{1}{4}\lambda \langle [a^{\dagger}_{-,m} a_{+,m} + a^{\dagger}_{-,m'} a_{+,m'}] \rangle. \tag{42}$$

Thus as promised the expectation value of an auxiliary field is a candidate order parameter of the symmetry in (39).

Our hamiltonian now takes the form

$$H = H_0 + \sum_{m,m'}{}' \left\{ \frac{2(\sigma_{m,m'})^2}{\lambda} + \frac{2(\sigma^{*}_{m,m'})^2}{\lambda} - \sigma_{m,m'} [a^{\dagger}_{+,m} a_{-,m} + a^{\dagger}_{+,m'} a_{-,m'}] \right.$$
$$\left. - \sigma^{*}_{m,m'} [a^{\dagger}_{-,m} a_{+,m} + a^{\dagger}_{-,m'} a_{+,m'}] \right\}. \tag{43}$$

As in the field theory, the effective potential $\mathscr{V}(\langle\sigma\rangle)$ is defined as the sum of all connected vacuum-to-vacuum diagrams with the expectation value, $\langle\sigma\rangle$, of the auxiliary fields allowed to be non-zero. The leading terms in the $1/N$ expansion of $\mathscr{V}(\langle\sigma\rangle)$ are given by the vacuum expectation energy of the auxiliary fields plus a sum of one-body one-loop diagrams i.e.

$$\mathscr{V}(\langle\sigma\rangle) = \sum_{m,m'}{}' \frac{2(\langle\sigma_{m,m'}\rangle)^2}{\lambda} + \frac{2(\langle\sigma^{*}_{m,m'}\rangle)^2}{\lambda}$$
$$+ \sum_{n} \frac{1}{2\pi i} \int d\omega \, e^{i\omega 0^{+}} \operatorname{Tr} \left\{ \tfrac{1}{2} [f_n(\omega) \mathscr{B}_n]^2 + \tfrac{1}{4} [f_n(\omega) \mathscr{B}_n]^4 + \cdots \right\}$$
$$+ O(1/N), \tag{44}$$

where $f_n(\omega)$ is the one-body Green for a particle(hole) having spin projection n

$$f_n(\omega) = \frac{1}{\omega - \mathscr{A}_n}, \tag{45}$$

with

$$\mathscr{A}_n = \begin{pmatrix} \tfrac{1}{2}\varepsilon - i0^{+} & 0 \\ 0 & -\tfrac{1}{2}\varepsilon + i0^{+} \end{pmatrix}. \tag{46}$$

The interaction matrix $\mathscr{B}_n$ has the form

$$\mathscr{B}_n = \begin{bmatrix} 0 & \Sigma_m [\langle\sigma_{n,m}\rangle + \langle\sigma_{m,n}\rangle] \\ \Sigma_{m'} [\langle\sigma^{*}_{n,m'}\rangle \langle\sigma^{*}_{m',n}\rangle] & 0 \end{bmatrix}. \tag{47}$$

The origin of the terms in the sum of (44) is easily seen. The first term is the Fourier transform of a particle undergoing the interaction $\mathscr{B}$ at time 0 propagating forwards to time t where it interacts via a second $\mathscr{B}$ whereupon it propagates backwards in time to the original $\mathscr{B}$ interaction at $t = 0$ which turns it back into the original state which started out (wherein the explanation for taking the trace). The convergence factor $e^{i\omega 0^+}$ is a result of avoiding an ambiguity of the time ordering operator at $t = 0$. The factor $\frac{1}{2}$ corrects for our ability to choose either of the $\mathscr{B}$ as the starting point. The second term in (44) describes a situation where the particle interacts with $\mathscr{B}$ three times before returning to the starting point and so on. Similar sums together with more detailed explanations of counting and convergence factors have been considered recently by Yang et al. [8].

Using the fact that the trace of any odd power of $f_n(\omega)\mathscr{B}_n$ is zero we can rewrite (44) as

$$\mathscr{V}(\langle\sigma\rangle) = \sum_{m,m'}{}' \left\{ \frac{2\big(\langle\sigma_{m,m'}\rangle\big)^2}{\lambda} + \frac{2\big(\langle\sigma^*_{m,m'}\rangle\big)^2}{\lambda} \right\}$$
$$+ \sum_n \frac{1}{2\pi i} \int d\omega\, e^{i\omega 0^+} \operatorname{Tr}\Big\{ f_n(\omega)\mathscr{B}_n + \tfrac{1}{2}\big[f_n(\omega)\mathscr{B}_n\big]^2$$
$$+ \tfrac{1}{3}\big[f_n(\omega)\mathscr{B}_n\big]^3 + \cdots \Big\} + O(1/N), \tag{48}$$

allowing us to write the one-loop sum (i.e. the third term on the right-hand side of (44)) as

$$-\sum_n \frac{1}{2\pi i} \int d\omega\, e^{i\omega 0^+} \operatorname{Tr} \ln\{1 - f_n\mathscr{B}_n\}. \tag{49}$$

This may be further rewritten by defining a Dyson equation

$$g_n = f_n + f_n\mathscr{B}_n g_n, \tag{50}$$

which allows us to write *

$$\mathscr{V}(\langle\sigma\rangle) = \sum_{m,m'}{}' \left\{ \frac{2\big(\langle\sigma_{m,m'}\rangle\big)^2}{\lambda} + \frac{2\big(\langle\sigma'_{m,m'}\rangle\big)^2}{\lambda} \right\}$$
$$+ \sum_n \frac{1}{2\pi i} \int d\omega\, e^{i\omega 0^+} \ln \operatorname{Det} g_n f_n^{-1}. \tag{51}$$

* It is interesting to note that had we carried out our calculation in the path-integral formalism we would have at one point integrated over the fermion fields in order to obtain an effective lagrangian. Such a procedure would have given us the same 'ln Det' form. Thus it is interesting to note how a path-integral manipulation can correspond to an infinite summation of Feynman graphs.

The one-loop sum may be evaluated by noting that g_n defined in (50) may be expressed

$$g_n = \frac{1}{\omega - \mathscr{A}_n - \mathscr{B}_n}. \tag{52}$$

The poles of (52) are obtained by solving the one-body eigenvalue equation,

$$[\mathscr{A}_n + \mathscr{B}_n]|\xi_n^\alpha\rangle = \xi_n^\alpha|\xi_n^\alpha\rangle. \tag{53}$$

In the Lipkin model case (53) has just two eigenvalues, denoted $\pm\xi_n$.

We now see that the determinant of (51) is simply expressed as

$$\mathrm{Det}\{g_n f_n^{-1}\} = \frac{[\omega + \frac{1}{2}\varepsilon - i0^+][\omega - \frac{1}{2}\varepsilon + i0^+]}{[\omega + \xi_n - i0^+][\omega - \xi_n + i0^+]}, \tag{54}$$

allowing us to write

$$\ln \mathrm{Det}\{g_n f_n^{-1}\} = \ln[\omega + \tfrac{1}{2}\varepsilon - i0^+] - \ln[\omega + \xi_n - i0^+] + \text{terms having poles in the lower } \omega\text{-plane}. \tag{55}$$

Under the ω-integration of (51), the terms having poles in the lower ω-plane are identically equal to zero. Introducing an integration variable x, the first two terms of (55) may be rewritten

$$\sum_n \int \mathrm{d}\omega \frac{\mathrm{e}^{i\omega 0^+}}{2\pi i} \int_0^1 \mathrm{d}x \frac{\frac{1}{2}\varepsilon - \xi_n}{\omega + \xi_n - i0^+ - x[\xi_n - \frac{1}{2}\varepsilon]}. \tag{56}$$

Inverting the order of integration and performing the contour integration first we have the surprisingly simple result for the one-loop diagram sum

$$\sum_n (\tfrac{1}{2}\varepsilon - \xi_n). \tag{57}$$

Results of a similar eigenvalue form were obtained by Tzeng and Kuo [9] in a somewhat different context for calculating sausage diagrams using particle–particle hole–hole ring diagrams.

For our Lipkin model hamiltonian, the one-body eigenmatrix for spin projection n is

$$\mathscr{A}_n + \mathscr{B}_n = \begin{bmatrix} \frac{1}{2}\varepsilon & \Sigma_m[\langle\sigma_{n,m}\rangle\langle\sigma_{m,n}\rangle] \\ \Sigma_{m'}[\langle\sigma^*_{n,m'}\rangle + \langle\sigma^*_{m',n}\rangle] & -\frac{1}{2}\varepsilon \end{bmatrix}, \tag{58}$$

and has solutions

$$\pm\xi_n = \pm\sqrt{\tfrac{1}{4}\varepsilon^2 + \sum_{m,m'} \big(\langle\sigma_{n,m}\rangle + \langle\sigma_{m,n}\rangle\big)\big(\langle\sigma^*_{n,m'}\rangle + \langle\sigma^*_{m',n}\rangle\big)}\,. \tag{59}$$

We thus find that

$$\mathscr{V}(\langle\sigma\rangle) = \sum_n \left\{ \sum_m \left(\frac{2\big(\langle\sigma_{n,m}\rangle\big)^2}{\lambda} + \frac{2\big(\langle\sigma^*_{n,m}\rangle\big)^2}{\lambda} \right) + \tfrac{1}{2}\varepsilon - \sqrt{\tfrac{1}{4}\varepsilon^2 + \sum_{m,m'} \big(\langle\sigma_{n,m}\rangle + \langle\sigma_{m,n}\rangle\big)\big(\langle\sigma^*_{n,m'}\rangle + \langle\sigma^*_{m',n}\rangle\big)} \right\}. \tag{60}$$

The minimum satisfies hermitivity conditions

$$\langle\sigma_{n,n'}\rangle = \langle\sigma^*_{n,n'}\rangle = \text{positive real}, \tag{61}$$

where the last assignment is chosen for convenience. In addition, the minimum satisfies the angular-momentum symmetry so we take

$$\langle\sigma_{n,n'}\rangle = \langle\tilde{\sigma}\rangle \qquad \text{for all } n,\ n'. \tag{62}$$

The effective potential thus acquires the simple form

$$\mathscr{V}(\langle\tilde{\sigma}\rangle) = \frac{4N(N-1)\langle\tilde{\sigma}\rangle^2}{\lambda} + \tfrac{1}{2}N\varepsilon - N\sqrt{\tfrac{1}{4}\varepsilon^2 + 4(N-1)^2\langle\tilde{\sigma}\rangle^2} + \mathrm{O}\big((1/N)^0\big). \tag{63}$$

The effective potential may be more conveniently written in terms of the rescaled interaction, v, and a rescaled field, σ, defined

$$\sigma \overset{\text{def}}{=} 2(N-1)\tilde{\sigma}, \tag{64}$$

and

$$v \overset{\text{def}}{=} (N-1)\lambda, \tag{65}$$

yielding

$$\mathscr{V}(\langle\sigma\rangle) = N\left(\frac{\langle\sigma\rangle^2}{v} - \big(\tfrac{1}{4}\varepsilon^2 + \langle\sigma\rangle^2\big)^{1/2} + \tfrac{1}{2}\varepsilon + \mathrm{O}(1/N) \right). \tag{66}$$

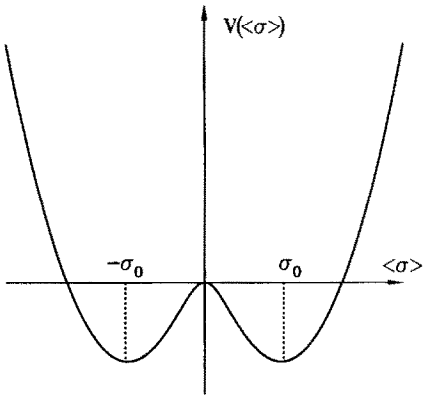

Fig. 3. The spontaneously broken effective potential for the Lipkin model plotted as a function of the expectation value of the auxiliary field, $\langle\sigma\rangle$.

Ignoring $1/N$ corrections, the minimization condition is now simply found to be

$$\left.\frac{d\mathscr{V}(\langle\sigma\rangle)}{d\langle\sigma\rangle}\right|_{\langle\sigma\rangle=\sigma_0} = \frac{2\sigma_0}{v} - \frac{\sigma_0}{\sqrt{\frac{1}{4}\varepsilon^2+\sigma_0^2}} = 0. \tag{67}$$

We see that there are two different domains of solutions to σ_0

$$\sigma_0 = \begin{cases} 0 & \text{if } \varepsilon \geqslant v \\ \sqrt{\frac{1}{4}(v^2-\varepsilon^2)} & \text{if } \varepsilon \leqslant v. \end{cases} \tag{68}$$

A typical (and familiar) example of the effective potential, (3.66), for $v > \varepsilon$ is shown in Fig. 3.

4. The RPA excitation spectrum

In order to construct an RPA matrix for the Lipkin model we must construct an angular-momentum-invariant particle–hole state. Our particle–hole state is then chosen to be

$$\sqrt{\tfrac{1}{2}}\, C^{j,j,0}_{m,-m,0}(-)^{j-m} a^{\dagger}_{+,m} a_{-,m}, \tag{69}$$

where the $\sqrt{\frac{1}{2}}$ is a normalization factor arising from the fact that we are concerned with identical fermions.

Using the procedure outlined in sect. 2 for the states given in (69), we easily find the RPA matrix for the Lipkin model

$$\begin{bmatrix} \varepsilon & v \\ -v & -\varepsilon \end{bmatrix}, \tag{70}$$

having eigenvalues

$$\Lambda = \pm\sqrt{\varepsilon^2 - v^2}\,. \tag{71}$$

We note that the eigenvalues of this RPA equation are real for $v < \varepsilon$ and complex for $v > \varepsilon$. Thus the Lipkin model provides an excellent example of the features mentioned in sect. 2. That is, above a certain coupling strength the eigenvalues become complex. Just before this point one can verify that the X and Y normalizations diverge. However, we saw in the previous section that the point of onset of complex eigenvalues, $v > \varepsilon$ is exactly the same as the point where our unperturbed vacuum becomes unstable and $\langle\sigma\rangle$ develops a non-zero expectation value. Thus RPA should be carried out about the true vacuum rather than the unstable perturbative vacuum.

For a given σ-vacuum the single-particle eigenstate is

$$\begin{bmatrix} \frac{1}{2}\varepsilon & \langle\sigma\rangle \\ \langle\sigma\rangle & -\frac{1}{2}\varepsilon \end{bmatrix}\begin{bmatrix} \alpha \\ \beta \end{bmatrix} = \xi\begin{bmatrix} \alpha \\ \beta \end{bmatrix}, \tag{72}$$

where $|\alpha|^2 + |\beta|^2 = 1$. Thus the particle state in the $\langle\sigma\rangle$ vacuum has a probability amplitude α to be in the particle state of the original vacuum, $\langle\sigma\rangle = 0$, and a probability amplitude β to be in the hole state of the original vacuum. The hole eigenstate on the other hand is

$$\begin{bmatrix} \frac{1}{2}\varepsilon & \langle\sigma\rangle \\ \langle\sigma\rangle & -\frac{1}{2}\varepsilon \end{bmatrix}\begin{bmatrix} -\beta \\ \alpha \end{bmatrix} = -\xi\begin{bmatrix} -\beta \\ \alpha \end{bmatrix}. \tag{73}$$

The probability amplitude for the particle–hole pair of the $\langle\sigma\rangle$ vacuum to be in the same state as the particle–hole pair of the $\langle\sigma\rangle = 0$ vacuum is therefore α^2. The probability amplitude to be in a two-hole state is $\alpha\beta$ and a two-particle state $-\alpha\beta$. Finally the probability amplitude to be propagating as a backwards particle–hole state is β^2.

Now we can calculate the matrix elements of the σ_0 particle–hole RPA. The matrix element for a particle–hole particle–hole interaction is $v(\alpha_0^4 + 2\alpha_0^2\beta_0^2 + \beta_0^4) = v$. That is, $v\alpha_0^4$ gives the interaction strength for the particle–hole particle–hole interaction proceeding exactly as for the $\langle\sigma\rangle = 0$ vacuum, $2v\alpha_0^2\beta_0^2$ the interaction strength for proceeding as a particle–particle hole–hole interaction of the $\langle\sigma\rangle = 0$ vacuum etc. Recalling that the one-body energies for the σ_0-vacuum are $\pm\xi_0 = \pm\sqrt{\frac{1}{4}\varepsilon^2 + \sigma_0^2}$, we form the RPA equation for the σ_0-vacuum

$$\begin{bmatrix} \sqrt{\varepsilon^2 + 4\sigma_0^2} & v \\ -v & -\sqrt{\varepsilon^2 + 4\sigma_0^2} \end{bmatrix}. \tag{74}$$

where σ_0 is given in Eq. (68).

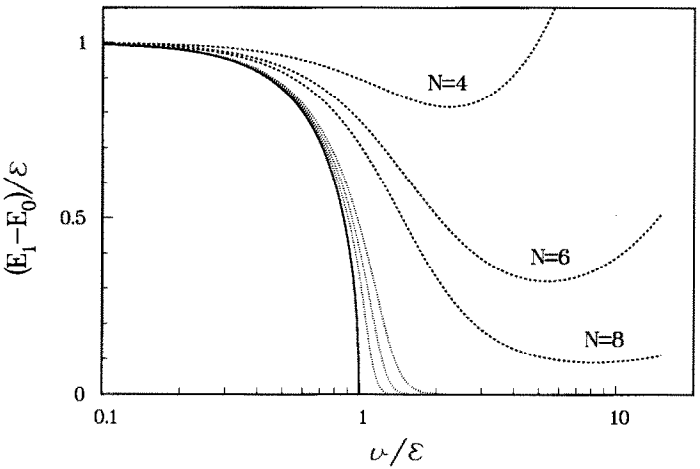

Fig. 4. Energy of the first excited state, E_1, with respect to the ground state, E_0, plotted as a function of interaction strength, $\upsilon = \lambda(N-1)$. The solid line is the RPA, (i.e. $N \to \infty$), limit as given by Eq. (71). The dotted curves are given respectively by the solutions at $N = 30$, $N = 50$, $N = 100$.

In the case of $\upsilon < \varepsilon$, $\langle \sigma \rangle = 0$; Eq. (74) is none other than the ordinary RPA equation given by the techniques of sect. 2 (i.e. Eq. (70)). For $\upsilon > \varepsilon$, Eq. (74) has zero eigenvalues indicating that the first excited state has collapsed into degeneracy with the ground state. This indicates that our model system undergoes a phase transition from a phase having a non-degenerate ground state to a phase having a degenerate ground state at $\upsilon = \varepsilon$. The eigenspectrum of Eq. (68) is plotted in Fig. 4 together with the exact solutions for $N = 4, 6, 8, 30, 50, 100$. Keeping in mind that all the plots that touch the zero excitation axis remain there, then we see it is

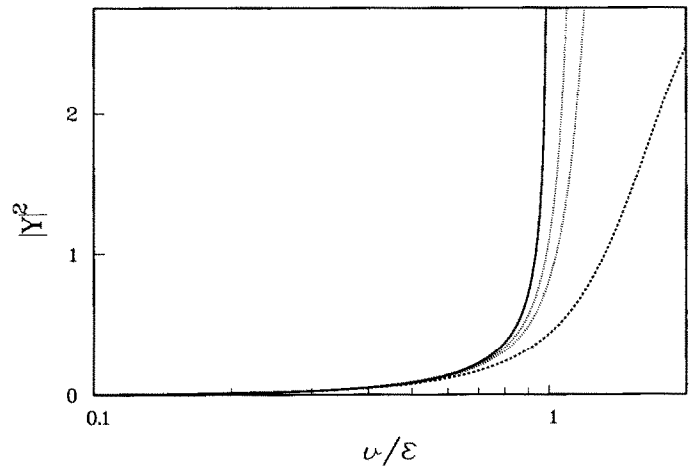

Fig. 5. The transition amplitude normalization, $|Y|^2$, plotted as a function of interaction strength. The RPA limit is given by the solid curve, $N = 14$ by the dashed curve, $N = 50$ and $N = 100$ by dotted curves.

highly suggestive that RPA together with the effective potential provides the exact $N \to \infty$ limit.

The reader should note that for this simple system ordinary RPA yields the $N \to \infty$ limit up to the transition point, $v = \varepsilon$. Secondly, by introducing an auxiliary field, we take into account the spontaneous generation of a single-particle potential $\langle \sigma \rangle$ which prevents complex eigenvalues and accurately describes the creation of a degenerate ground state for the regime $v > \varepsilon$.

We are now in a position to check the applicability of the RPA normalization derived in sect. 2 (see Eqs. (33) and (28)). Plotting the results for $N = 14$, $N = 50$, and $N = 100$, in Fig. 5, we are not surprised to see RPA yielding the appropriate $N \to \infty$ limit. This graph confirms a well-known rule of RPA analysis that one can only trust RPA normalizations when $|Y|^2$ is small. The reason is now clear. When $|Y|^2$ is large we are approaching the $N \to \infty$ phase transition point and thus $1/N$ corrections (i.e. extended RPA) become very important.

5. Binding energy and single-particle spectrum

Let us now look at other important physical quantities such as the ground-state energy and single-particle excitation spectrum.

We start with the true ground-state energy E_0. The standard analysis tells us that the energy of the true ground state with respect to the perturbative ground state, $\Sigma_0 = E_0 - \epsilon_0$, is given by

$$\mathscr{V}(\langle \sigma \rangle)|_{\langle \sigma \rangle = \sigma_0}. \tag{75}$$

Of course we have calculated $\mathscr{V}$ only to leading order in $1/N$, i.e. order $(1/N)^{-1}$. The next order in $1/N$ are diagrams of order $(1/N)^0$. Thus we expect the correlation energy, Δ, defined in the current work as the difference between the true ground-state energy shift, Σ_0 and Eq. (75) calculated to lowest order $1/N$, to approach some finite function of v as $N \to \infty$.

Such indeed appears to be the case as shown in Fig. 6 where we plot results for $N = 14$, 100, 200. Note that as in variational treatments our result always underestimates the total binding energy. Using techniques similar to those of ref. [9] we can calculate to all orders in v the correlation diagrams (sausage diagrams) for $v < \varepsilon$ which form the first-order $1/N$ corrections (also plotted in Fig. 6). Unfortunately, we know of no convenient all-order sums for the case where $v > \varepsilon$. As expected this correlation energy, Δ, has a peak at the transition point, $v = \varepsilon$. That the correlation then increases at large v can be attributed to the fact that the energy scale of the system is increasingly going beyond the unperturbed reference

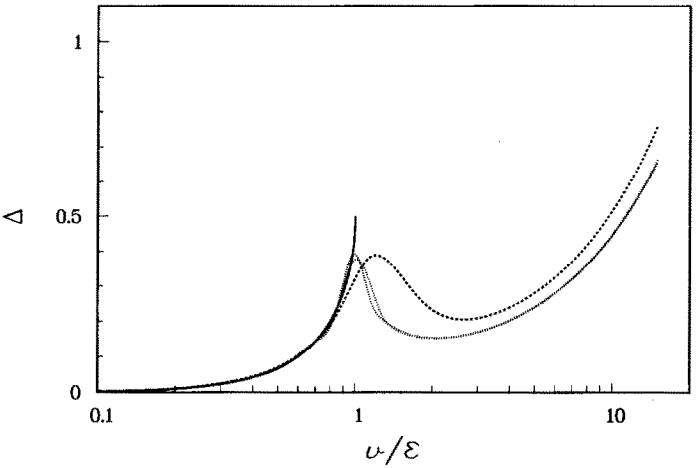

Fig. 6. Correlation energy of the ground state plotted as a function of interaction strength. $N = 14$ is the dashed curve, $N = 100$ and $N = 200$ are given by dotted curves, $N = 200$ having the highest peak. The calculated first-order $1/N$ correction for $\upsilon < \varepsilon$ is given by the solid curve.

energy ε. An analogous behavior for Δ is found in the usual Hartree–Fock mean-field analysis [10].

The single-particle energy can be similarly compared with the exact results. Single-particle Green function theory tells us that the single-particle energy is given by the Landau–Migdal relation of

$$E_{\mathrm{sp}} = E_0^{N+1} - E_0^N, \tag{76}$$

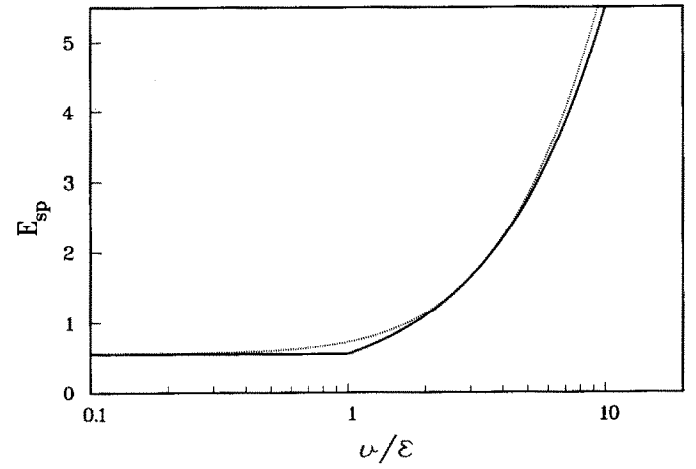

Fig. 7. Single-particle energies, $E_{\mathrm{sp}} \overset{\mathrm{def}}{=} E_0^{N+1} - E_0^N$, plotted as a function of interaction strength. The solid curve gives the $N \to \infty$ limit. The $N = 4$ solution is given by the dotted curve.

where both E_0^{N+1} and E_0^N are calculated for the N-particle Lipkin model. That is, E_0^{N+1} in the absence of interaction would be the energy of N-particles in the filled $-\frac{1}{2}\varepsilon$ shell plus one particle in the $\frac{1}{2}\varepsilon$ shell, while E_0^N would be the energy of the filled $-\frac{1}{2}\varepsilon$ shell, thus given an unperturbed single-particle energy of $E_{sp} = \frac{1}{2}\varepsilon$. The exact result for $N = 4$ is plotted in comparison with the $N \to \infty$ limit in Fig. 7. As we see, these results are already in rather good agreement. $N = 6$ is already so close to the $N \to \infty$ limit that it is only distinguishable near $v = \varepsilon$. Even this small discrepancy rapidly disappears and at $N \gtrsim 20$ no difference can be seen on the scale shown here.

6. Discussion

We note that the behavior of the excitation spectrum in Fig. 4 is precisely what we would expect based on the effective potential. As long as $v < \varepsilon$, the effective potential has a unique minimum, and the RPA gives the location of the first excited state. For $v > \varepsilon$, the effective potential has a double minimum, and thus a doubly degenerate ground state. In other words this is the discrete symmetry analogue of the Goldstone phenomenon. An analogous phenomenon also appears in the Gross–Neveu model [11]. There the spontaneous breaking of a discrete chiral symmetry results in a scalar bound state having the same energy as a free fermion–antifermion pair.

It is interesting to note that the effective potential of Eq. (66) only depends on the parameter v/ε. Thus naively one would expect SSB for all N. One quickly realizes however that the height of the potential barrier (see Eq. (66)) between the two "degenerate" states is proportional to N, and thus we can expect a tunneling phenomenon at finite N. As such we might consider using the WKB approximation, i.e. instantons, to estimate the tunneling effects [12]. Rather than carry out such a program (we will address this problem quantitatively using a different method in a subsequent publication) let us simply look qualitatively at the finite N effects based on the exact solution.

For $N > 8$ the point of (near) degeneracy is simply pushed out beyond $v = \varepsilon$. However, for $N \leqslant 8$ tunneling prevents the formation of a degenerate state. From Eq. (42) we identify the condensate as

$$\langle a^\dagger_{+,m} a_{-,m} \rangle = \alpha_0 \beta_0 = \frac{\sigma_0}{v}, \tag{77}$$

where m is arbitrary. The first equality is found simply by taking the true ground state to be a scalar determinant of hole eigenstates in the σ_0 "mean" field, (73). The second is found by using the constraint equation (42). We find from the exact solutions that this condensate is zero for all values of v at finite N provided the ground and first excited states are non-degenerate. In the degenerate case we are

allowed to construct a superposition state where (77) is non-zero. Thus in accordance with a discrete version of Goldstone's theorem the symmetry can be spontaneously broken only when a ground-state degeneracy is created.

In principle the ground state and first excited state are never degenerate at finite N. Although they become infinitesimally close as $v \to \infty$. Thus it would appear that in a complete theory of the effective potential that SSB would apparently occur at finite N for the physical modes, while the underlying symmetry of the bare fields is never broken at finite N.

We remind the reader that this model is very reminiscent of the Gross–Neveu model. There one has an $O(N)$ symmetry where N is the number of fundamental fermions, plus a discrete chiral symmetry. In the $1/N \to 0$ limit, one readily obtains the prediction of spontaneous symmetry breaking with an accompanying degeneracy of the ground state and the first excited state. The biggest apparent difference between the behavior of the two models is that in the Lipkin model SSB only occurs when v is sufficiently large. This however only occurred because we gave the hamiltonian an unperturbed single-particle spectrum. Had the two unperturbed levels been degenerate from the outset then all values of v (in the $N \to \infty$ limit) would have generated SSB. Simultaneously, a non-degenerate single-particle spectrum (the non-relativistic analogue of mass generation) would be generated.

Finally we note that these techniques can be generalized to more realistic nuclear models. In a realistic calculation the N counts the number of degenerate or nearly degenerate loops to be summed over in the RPA calculation. This work would seem to imply that as long as N is sufficiently large, we might expect $1/N \to \infty$ results to be reasonably accurate for most quantities. As is well known however, the accurate evaluation of physical quantities such as binding energies will often necessitate the calculation of $1/N$ corrections.

Careful study of the use of auxiliary fields shows that this method is closely related to the Hartree–Fock method. In some circumstances the two methods are identical. In realistic cases a combined use of the two methods may prove the most useful. For instance the ease with which we solved the Lipkin model auxiliary potential was due in large part to the fact that eigenstates of the one-body H_0 potential always form a stationary point solution (local maximum or minimum), of the Hartree–Fock equations. Thus a realistic potential may be best solved by finding the Hartree–Fock solution and then using auxiliary fields to probe for deformation instabilities.

We would also like to point out a recent work wherein RPA was formulated in a variational context [10], and improvements were made by making improved approximations to a general variation. This method proved quite reliable in providing ground-state properties for all values of v excepting those near the transition point where it still was an improvement with respect to other methods. Although we concentrated here on the $1/N$ expansion, the relationship between these techniques may prove of interest.

The zero-temperature analysis of this work is currently being extended to finite temperature where phase transitions and symmetry restoration may be properly discussed.

The author would like to thank Manque Rho, D. Vautherin, Dan Strottman, and T.T.S. Kuo for helpful discussions.

References

[1] H.J. Lipkin, N. Meshkov and A.J. Glick, Nucl. Phys. 62 (1965) 188
[2] P. Ring and P. Schuck, The nuclear many-body problem (Springer, Berlin, 1980)
[3] E. Witten, Nucl. Phys. B145 (1978) 110
[4] W. Hengeveld, W.H. Dickhoff and K. Allaart, Nucl. Phys. A451 (1986) 269
[5] M.G.E. Brand, K. Allaart and W.H. Dickhoff, Nucl. Phys. A509 (1990) 1
[6] S.D. Yang and T.T.S. Kuo, Nucl. Phys. A456 (1986) 413
[7] K.T. Chiang and T.T.S. Kuo, Equation of state and critical behavior of the finite temperature RPA, *in* Lectures presented at the Spring School on medium and high-energy nuclear physics, 1991, Tainan Taiwan R.O.C. p. 457
[8] S.D. Yang, J. Heyer and T.T.S. Kuo, Nucl. Phys. A448 (1986) 420
[9] Y. Tzeng and T.T.S. Kuo, Nucl. Phys. A485 (1988) 85
[10] J. Dukelsky and P. Schuck, Nucl. Phys. A512 (1989) 466
[11] D.J. Gross and A. Neveu, Phys. Rev. D10 (1974) 3235
[12] S. Coleman, Aspects of symmetry: Selected Erice lectures, ch. 7: Uses of Instantons (Cambridge Univ. Press, Cambridge, 1985) p. 265
[13] J. Zinn-Justin, Quantum field theory and critical phenomena (Oxford Univ. Press, Oxford, 1990)
[14] P.J. Ellis, Nucl. Phys. A467 (1987) 173